CHAPTER V

SILK SERICIN/CLAY AEROGEL NANOCOMPOSITES

5.1 ABSTRACT

The aim of this study was to prepare silk sericin/clay aerogel, the highly porous biodegradable material, by freeze-drying process. Due to silk sericin/clay aerogel formed fragile material hence poly(vinyl alcohol) was employed to improve the mechanical properties. Silk sericin (*Bombyx mori*) was extracted from Thai silk cocoon, Nang Noi. After that, the silk sericin/PVA/clay aerogel was prepared by varying silk sericin content in 1, 2, 3 and 4 % by weight and clay was introduced in 2, 4, 6, and 8% by weight in order to study the effect of silk sericin and clay contents to the properties of the aerogel. The dispersion of clay in aerogel and morphology of silk sericin/PVA/clay aerogel was determined by X-ray Diffractometer (XRD) and Field Emission Scanning Electron Microscope (FE-SEM), respectively. The mechanical and thermal properties were investigated by Universal Testing Machine (LLOYD) in compression mode and Thermogravimetric-Differential Thermal Analyzer (TG-DTA), respectively. The XRD results indicted the intercalation of polymer in the clay palates. FE-SEM micrographs presented the "house of cards" structure with interconnected pore. The mechanical and thermal properties directly depended on clay and silk sericin contents. By increasing clay contents, the mechanical properties were improved but thermal properties were dropped due to the oxidation of ferric ion effect. The increasing of silk sericin content strongly improved the mechanical and thermal properties of the aerogels.

Keywords: Sericin; Silk; Clay aerogel; Aerogel; Porous structure

5.2 INTRODUCTION

Silk sericin (SS) is the hydrophilic glue like protein produced from the mulberry silk worm (*Bombi Mori*) composed around 20-30% of the silk cocoon. In the silk industry, several tons of silk sericin must be removed from the raw silk by

"degumming process" and leaved in processing silk wasted water resulting in environmental water pollution (Zhang, 2002). Silk sericin is an invaluable product but to be useful in many applications ranged from the cosmetics to biomedical including wound dressing and cell culture additives. Many researchers suggested that silk sericin can enhance cell growth and can be used for the cell culture application such as Takeuchi and coworkers (2005) used silk sericin coated on the porous structure of alpha-tricalcium phosphate to enhance bone regeneration and bone density in rabbit. Furthermore, Sarovart *et al.* (2003) reported antioxidant, antimicrobial and antifungus acitivities of silk sericin which can be used in daily life such as air filter treatment.

The smectite clay such as sodium montmorillonite and bentonite are extensively used to develop polymer/clay nanocomposites due to their characteristic properties such as high surface area, high aspect ratio and relatively low cost. When layered silicate clay pass through the environmental friendly process called freeze-drying, clay powder can be rearranged to the "house of cards" structure and this material is called "clay aerogel" (Bandi, 2006). Clay aerogel is the high porosity, low density, lightweight materials which is in the formed 3 dimension structure. This porous structure makes clay aerogels suitable for wide range applications like absorbent materials, insulator materials or biomedical materials including drug control release system and 3D-scaffold application. Many researchers interested in combined clay aerogel into biological application including scaffold for tissue engineering. However, neat clay aerogel is fragile and exhibited low mechanical properties. To overcome this problem the combination with polymeric materials is required (Bandi, 2006, Pojanavaraphan, 2010, Haroun, 2009).

In this study, the silk sericin/PVA/clay aerogel was prepared by freeze-drying process. Poly(vinyl alcohol) or PVA, synthetic polymer with good biocompatibility, was employed to improve the mechanical properties of aerogels because of the fragility of neat silk sericin/clay aerogel which occurred from the amorphous structure of silk sericin. Silk sericin was extracted from local Thai silk cocoon; Nang Noi. The silk sericin/PVA/clay aerogel was prepared by varied of silk sericin and clay contents in order to study the effect of silk sericin and clay on the properties of the aerogel. The silk sericin/PVA/clay aerogel was studied on structure, morphology,

mechanical and thermal properties by using XRD, FE-SEM, Universal testing machine, and TG-DTA, respectively.

5.3 EXPERIMENTAL

5.3.1 Raw materials

Thai silk cocoons (Nang Noi) were purchased from local Thai silk sericulture. Sodium-bentonite clay (Na-MMT), with cationic exchange capacity (CEC) of 49.74 meq/100 g clay, was kindly supplied from Thai Nippon Co.,Ltd, Thailand. Poly(vinyl alcohol) was purchased from KURARAY POVAL with average molecular weight at 9000-10000 (characterized by GPC) , hydrolyzed at 87-89 mol% and viscosity is 40-48 mPa.s (in 4% aqueous solution at 20°C)

5.3.2 Extraction of silk sericin

Silk sericin was extracted by using hot water degumming process. In detail, silk cocoons were cut in to small pieces (about 0.5×0.5 cm^2) and mixed with 300 ml. of purified water. Silk cocoon were autoclaved under high pressure at 120 °C for 1 hr. The fibroin was filtered out to obtain the silk sericin solution. Then, silk sericin solution was frozen in the glass shells at -40°C for 12 hr and was attached to a freeze-dryer maintained at -110°C for 48 hr to obtain silk sericin powder.

5.3.3 Preparation of silk sericin/PVA/clay aerogel

PVA (5 wt%) and silk sericin powder with various contents (1-4 wt%) were dissolved in purified water heated at 90°C with constant stirring until they were completely dissolved. Na-bentonite with different concentration (2-8 wt%) was added to the above mixture followed by vigorous stirring for 2 hr. Then, the mixtures were immediately frozen in cylindrical glass vials at -40°c for 12 hr and were attached to a freeze-dryer maintained at -110°C under vacuum for 48-72 hr to sublime the ice out.

The samples were coded CxPVA5SSy where x corresponds to clay content (wt%) and y corresponds to silk sericin content (wt%). For example, C8PVA5SS1 would compose of clay 8 wt%, PVA 5 wt% and silk sericin 1 wt%.

5.3.4 Characterizations

5.3.4.1 Density measurment

The density of the silk sericin/PVA/clay aerogels was calculated by mass and dimension measurement using Sartorius BS 224 S analytical balance and digital vernier caliper according to an equation:

$$\rho = \frac{M}{V} \qquad \text{(eq. 5.1)}$$

where ρ is mass density (g/cm^3), M is mass of sample (g) and V is volume of sample (cm^3).

5.3.4.2 Field Emission Scanning Electron Microscope (FE-SEM)

Field Emission Scanning Electron Microscope (Hitachi S-4800) was used to study the morphology of silk sericin/PVA/clay aerogel. The samples were coated with platinum under vacuum. FE-SEM micrographs were taken with the magnification range between 45-20.0k using an accelerator voltage of 2.0 kV.

5.3.4.3 Universal Testing Machine (LLOYD)

The mechanical properties of silk sericin/PVA/clay aerogel were determined by Universal testing machine (LLOYD) in compression mode with 500 N load cell at constant crosshead speed of 1 mm/min. The samples were prepared in the cylindrical shape with ~20 mm in diameter and height. Five samples of each composition were tested for reproducibility. The initial compressive modulus was calculated from the slope of the linear portion of the stress-strain curve.

5.3.4.4 Thermogravimetric-Differential Thermal Analyzer (TG-DTA)

Thermal stability of silk sericin/PVA/clay aerogels was determined by Thermogravimetric-Differential Thermal Analyzer (Perkin-Elmer Pyris Daimond thermogravimatric analysis). The weight of sample was in the range of 3-5 mg. and was heated at the heating rate of 10°C/min from 30-900°C in nitrogen atmosphere with nitrogen flow of 30 ml/min.

5.3.4.5 X-ray Diffractometer (XRD)

The structure of the silk sericin/PVA/clay aerogels were characterized by Bruker AXS Model D8 Discover X-ray diffractometer. The X-ray beam was Cu (k = 0.15406 nm) and the radiation operated at a tube voltage of 40 kV using a tube current of 30 mA. The samples were scanned in a step mode at a scan rate of 2°/min from 2θ = 5°–30°. The interlayer spacing (d_{001}-spacing) was calculated via the Bragg equation:

$$\lambda = 2d \sin\theta \qquad \text{(eq.5.2)}$$

where λ is the X-ray wavelength, d is the interlayer spacing, and θ is the diffraction angle.

5.3 RESULTS AND DISCUSSION

5.3.1 Appearance of silk sericin/PVA/clay aerogels

While smectite clay was dispersed in water, in this study was bentonite, the sol-gel phenomena was occurred by the edge-face conformation owing to the opposite electrostatic charges of faces and edges of clay plates. The faces have negative charges on siloxane surfaces and the edges have positive charges of alumina sheets resulting in the charge attraction. Layered clays could be rearrangement from the granular powder to the "house of cards" like structure by freeze-drying technique. When clay gel was frozen, the ice crystals were growing and push the clay particles aside to encourage the parallel orientation (Pojanavaraphanet *et al.*, 2008 and Bandi, 2006). After sublimed the ice out under vacuum, the house of cards structure was still maintained and leaved the layer interconnected pore which fulfill by the air. The schematic model described the formation of silk sericin/PVA/Na-bentonite aerogel is shown in Figure 5.1.

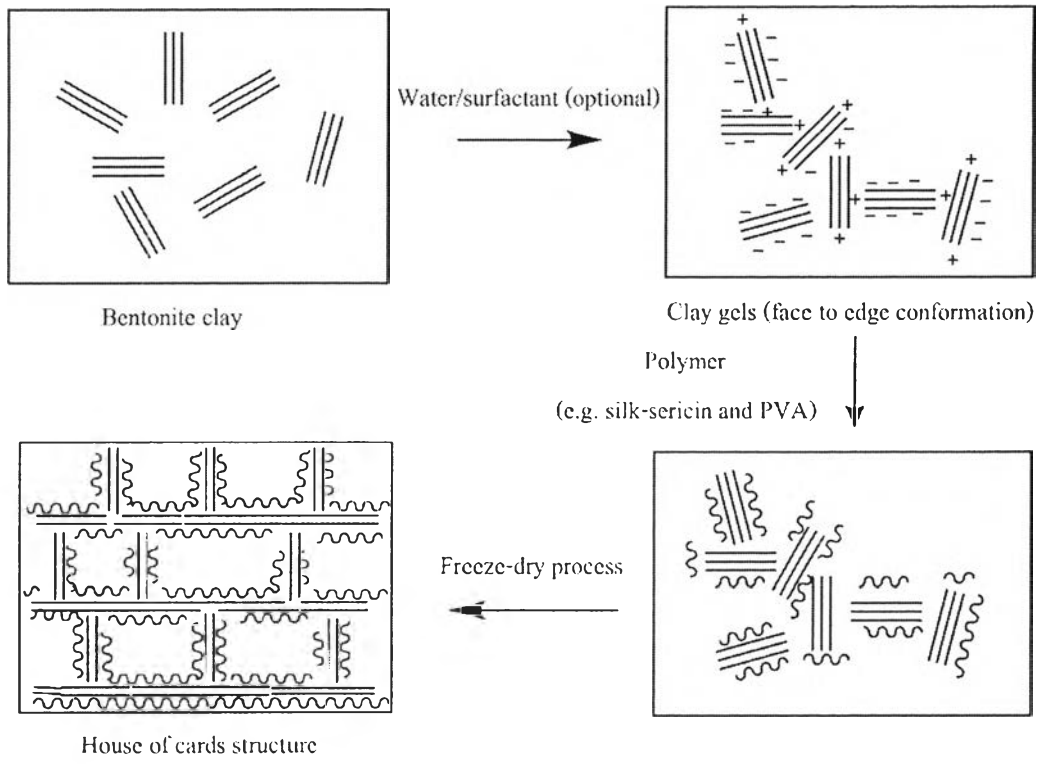

Figure 5.1 Schematic model suggested the formation of silk sericin/PVA/Na-bentonite aerogels.

Silk sericin/clay aerogels with freezing temperature at -40°C are shown in figure 5.2a and 5.2b. The silk sericin/clay aerogels showed the lamella porous obviously. Nevertheless, silk sericin/clay aerogels were formed fragile materials hence they were not appropriate for many applications because they were difficult to handle and had low mechanical properties. Due to silk sericin is an amorphous random coil natural polymer which exhibited low mechanical properties and neat clay aerogel is formed delicate material hence clay aerogel which cooperated with silk sericin revealed the characteristic properties of these two raw materials. To overcome this limitation, the PVA was employed so as to improve the mechanical properties of silk sericin/clay aerogels. Figure 5.2c and 5.2d show the silk sericin/PVA/clay aerogels. With only 3wt% of PVA, the physical appearance of the aerogel was changed from high roughness surface to smooth surface and the cracking of the aerogel was not observed.

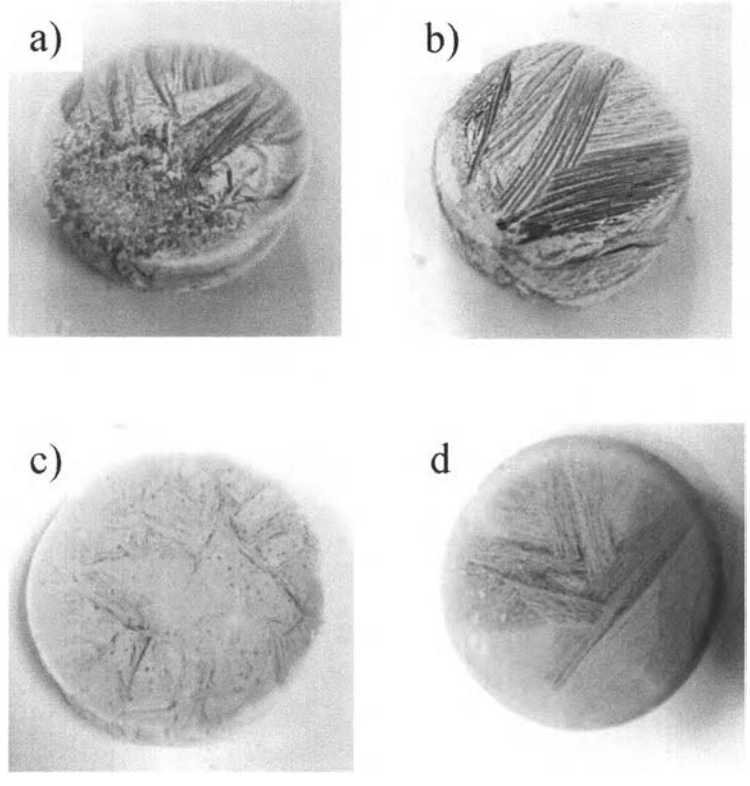

Figure 5.2 The physical appearance of (a), (b) silk sericin/clay aerogels, and (c), (d) silk sericin/PVA/clay aerogels.

Table 5.1 Density of silk sericin/PVA/clay aerogels with various clay and silk sericin contents

Samples	Density (g/cm^3)
C2PVA5SS1	0.12±0.004
C4PVA5SS1	0.09±0.012
C6PVA5SS1	0.11±0.003
C8PVA5SS1	0.11±0.020
C6PVA5SS2	0.13±0.007
C6PVA5SS3	0.14±0.004
C6PVA5SS4	0.15±0.002

Neat clay aerogel exhibited low density material with bulk density around 0.01-0.1 g/cm^3. Table 5.1 showed the density of silk sericin/PVA/clay aerogel. Silk sericin/PVA/clay aerogels presented the density ranged between 0.11-0.15 g/cm^3 depended on the composition of the aerogels. Increasing of silk sericin from 1-4 wt% content, the density slightly increased from 0.11 to 0.14 g/cm^3 because silk sericin was fulfilled the cavity between layers of clay lead to the denser material. Clay content was not outstandingly affected on the density of the aerogels.

5.3.2 Morphology of silk sericin/PVA/clay aerogel

FE-SEM micrographs of neat Na-bentonite aerogels with different magnitude are shown in Figure 5.3a and 5.3b. After freeze-drying, neat Na-bentonite formed the lamella structure like the "house of cards" structure which was duplicate of the ice crystal morphology (Gawryla *et al.*, 2009).

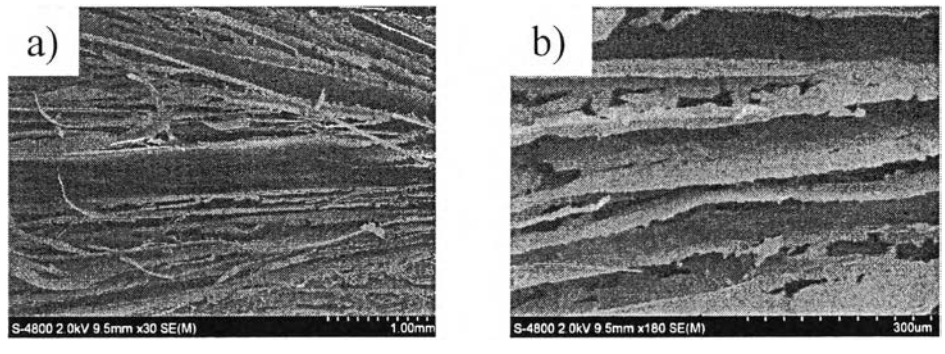

Figure 5.3 FE-SEM micrographs of neat Na-MMT aerogels at 8 wt% of clay.

The silk sericin/PVA/clay aerogels showed the lamella morphology similar to neat Na-bentonite aerogels but the clay layers were covered by silk sericin and PVA. In the case of aerogels with 2 and 4 wt% of clay (Figure 5.4a and 5.4b), the contents of clay were enough to produce the lamella structure but it was not obviously observed because each layer was highly covered by polymer and layers appear to be connected by webs of polymer resulting in the decreased in the distance between each layer and porosity (Gawryla *et al.*, 2008). In the case of aerogels with 6 and 8 wt% of clay (Figure 5.4c and 5.4d), the lamella morphology was clearly observed with lower amount of polymer webs linked between layers. The contents of

clay not only played an important role for produced clay aerogel structure but also affected to the distance between layers and pores size. To achieve the aerogel structure by freeze-drying process, around 1.4-2.9 wt% of clay was required (Somlai *et al.*, 2006). For aerogel with 8 wt% of clay, the clay gel dispersion was to viscous and difficult to process resulting in non-homogenous dispersion of the aqueous clay gel precursor hence the increasing of structure defects such as air bubbles was occurred (Figure 5.5) led to reducing of the mechanical properties of the aerogel. The air bubbles were not observed in the case of aerogel with clay content below 8 wt%. Somlai *et al.*, 2006 suggested that above 2.9 wt% of clay concentration was viscous and difficult to blend but Pojanavaraphan *et al.*, 2010 reported the clay content up to 7 phr (~ 6.7 wt%) still gave the good mechanical properties.

Not only clay content affected on the morphology of the aerogel but silk sericin also strongly influenced to the morphology of the aerogels. By increasing of silk sericin content, the lamella structure was not visibly observed owing to the high content of silk sericin which fulfill in the porous structure resulted in the decreasing the distance between layer and pore porosity. Figure 5.6 shows the FE-SEM micrographs of silk sericin/PVA/clay aerogel with different silk sericin contents. While increasing silk sericin content from 1 to 4 wt%, each layer of clay was thicker and each layer appeared to be connected by web of silk sericin and PVA. Figure 5.7a and 5.7b present the silk sericin and PVA on the surface of clay templates with different magnitude.

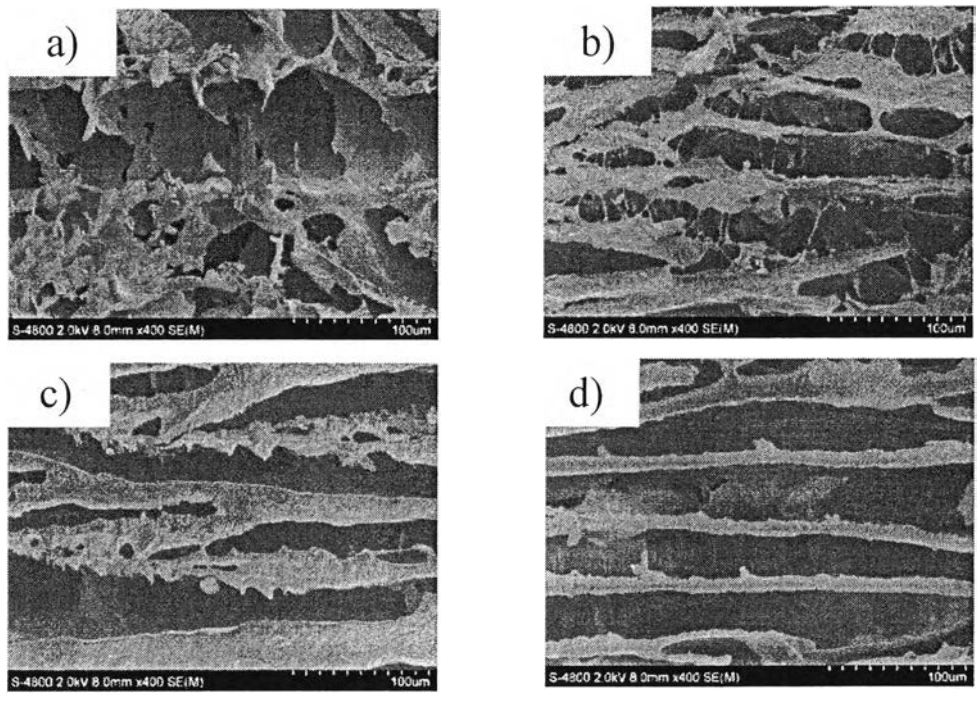

Figure 5.4 FE-SEM micrographs of silk sericin/PVA/clay aerogels (a) C2PVA5SS1, (b) C4PVA5SS1, (c) C6PVA5 SS1 and (d) C8PVA5SS1.

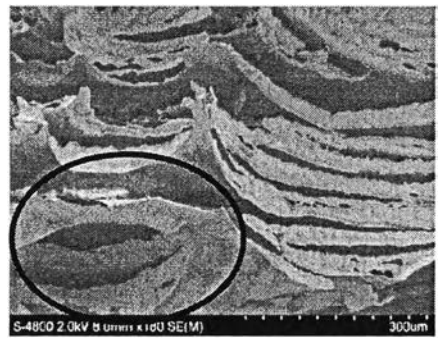

Figure 5.5 FE-SEM micrograph of C8PVA5SS1 with trapped air bubbles.

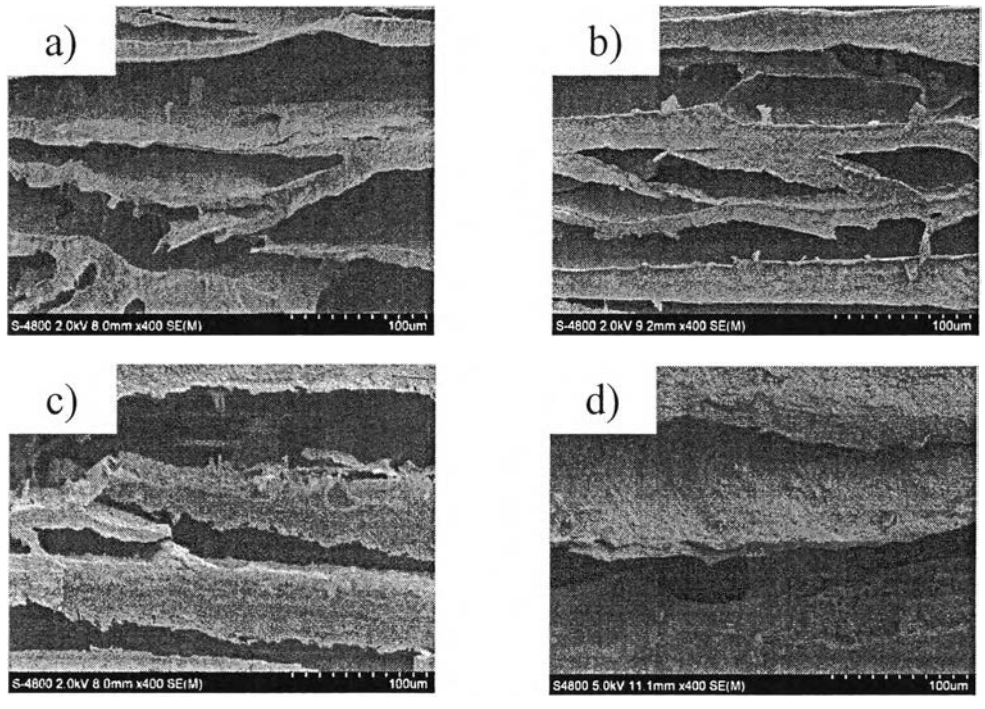

Figure 5.6 FE-SEM micrographs of silk sericin/PVA/clay aerogels (a) C6PVA5SS1, (b) C6PVA5SS2, (c) C6PVA5SS3 and (d) C6PVA5SS4

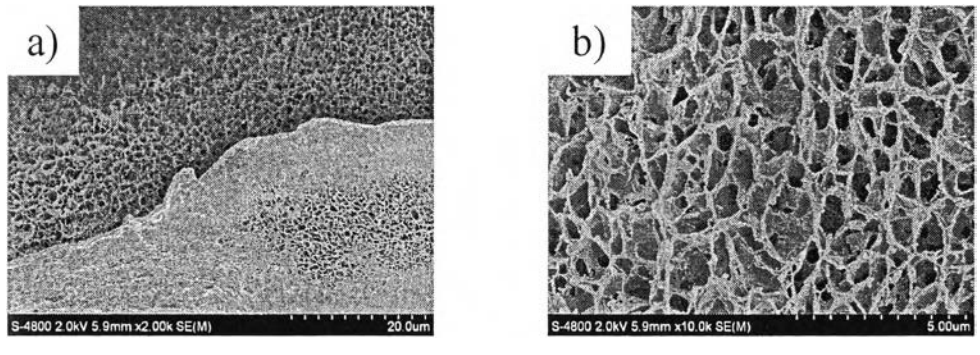

Figure 5.7 FE-SEM micrographs of silk sericin/PVA on the surface of clay templates in C8PVA5SS2.

The house of cards structure of silk sericin/PVA/clay aerogel exhibited highly porous with interconnected pore. This morphology was suitable for many applications, for example, absorbent materials, insulation material, cell culture

substrate, tissue engineering 3D scaffold and drug control release. For biomedical application, not only the porous structure of silk sericin/PVA/clay aerogels made it suitable for medical applications but also the good biocompatibility and the efficiency to promote cell growth of silk sericin were the good reasons.

5.3.3 Thermogravimetric-differential thermal analyzer

The effect of clay and silk sericin contents on the thermal properties were studied by thermogravimetric analysis. Figures 5.8-5.11 show the TGA and DTG thermograms of silk sericin/PVA/clay aerogels with various clay and silk sericin contents. The aerogels showed two main steps of weight loss. The first step observed up to 100 °C which corresponding to the evaporation of water (~2-3 % weight loss) followed by the second step started around 270 °C was associated with the decomposition of silk sericin (~260 °C) and PVA (~280 °C). The combination of bentonite clay in to the organic materials should be enhanced the thermal stability of the composites but in silk sericin/PVA/clay aerogel system, increasing of clay contents showed slight decreased in onset and peak decomposition temperatures. Morlat *et al.* (2004) suggested that the presence of ferric ion (Fe^{3+}) in octahedral sheet of clay could accelerate the thermal degradation of organic compound resulting in the reducing of thermal stability of the composite. According to Rangrong *et. al*, 2008, the element analysis of bentonite indicated the Ferric ions presented in the octahedral sheet of bentonite up to 1.09%.

On the other hand, thermal stability of the aerogels can be improved by increased silk sericin content because of the increasing number of strong hydrogen bonds between silk sericin, PVA molecules and silanol groups of clay bentonite (Teramoto *et al*, 2007). Additionally, the improving of thermal stability of the aerogels by increasing silk sericin loading was an indication that the silk sericin has the anti-oxidation property to inhibit the oxidation reaction of the ferric ion (Fe^{3+}). Table 5.2 and 5.3 summarizes the thermal behavior of silk sericin/PVA/clay aerogels with various clay and silk sericin contents.

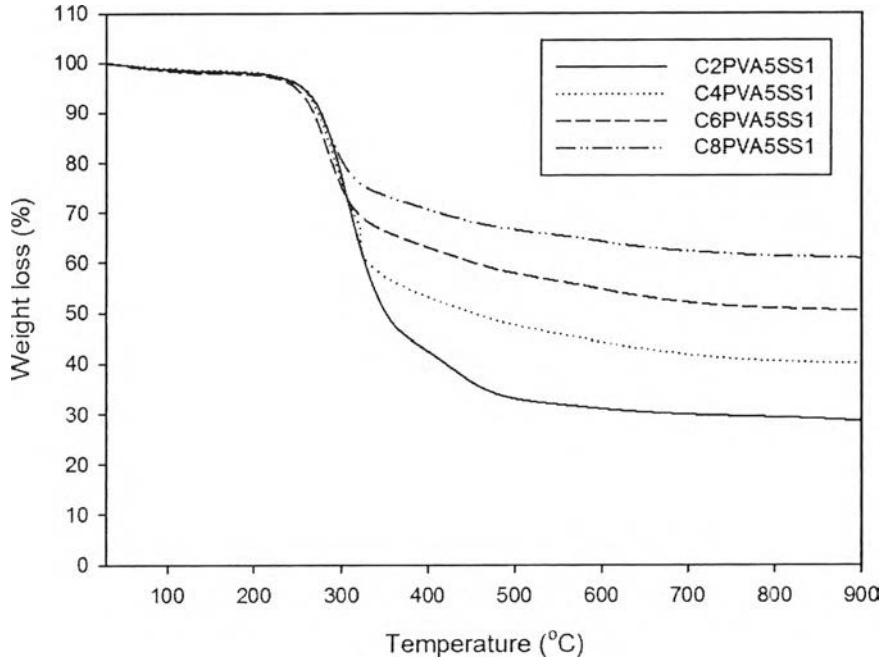

Figure 5.8 TGA thermograms of silk sericin/PVA/clay aerogels with various clay contents.

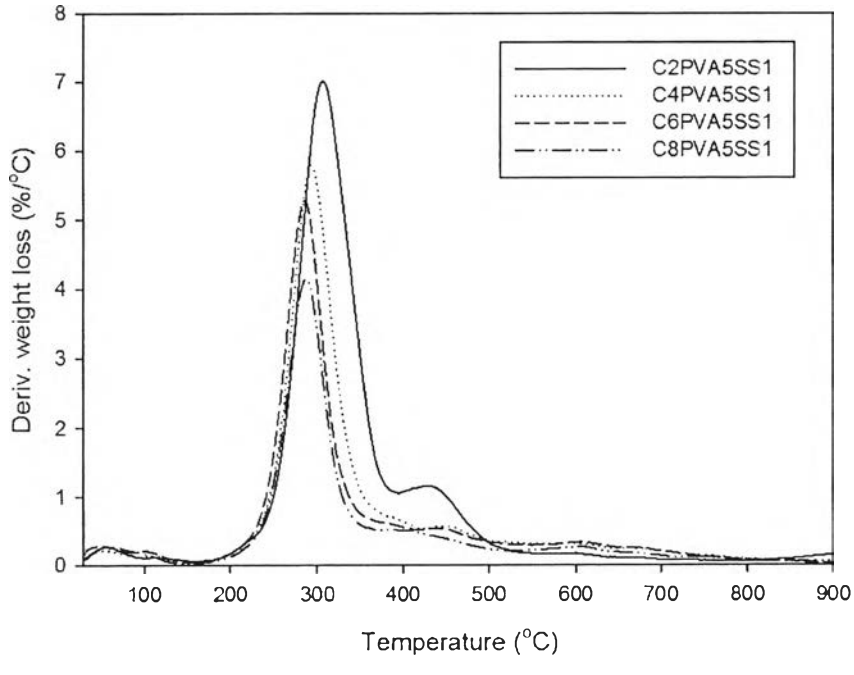

Figure 5.9 DTG thermograms of silk sericin/PVA/clay aerogels with various clay contents.

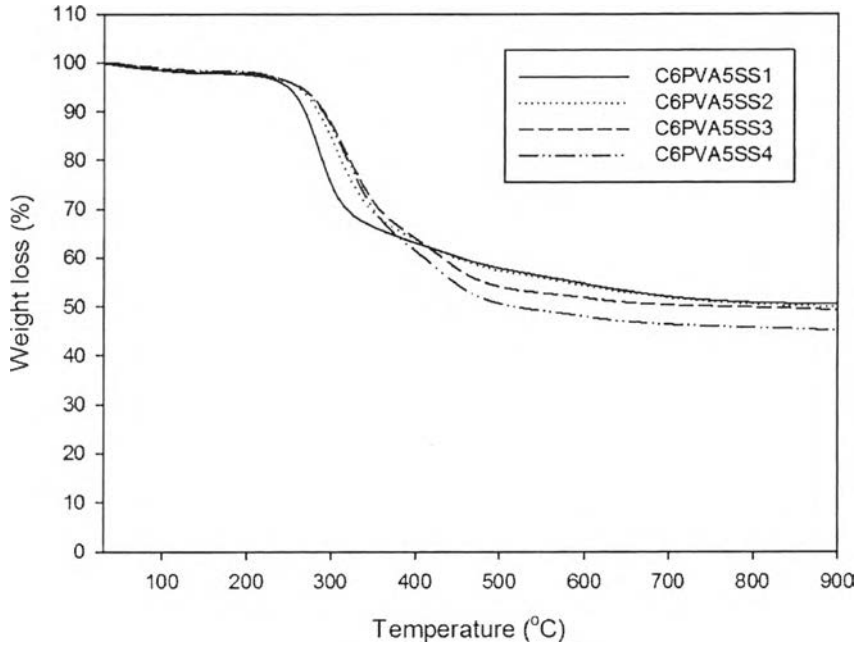

Figure 5.10 TGA thermograms of silk sericin/PVA/clay aerogels with various silk sericin contents.

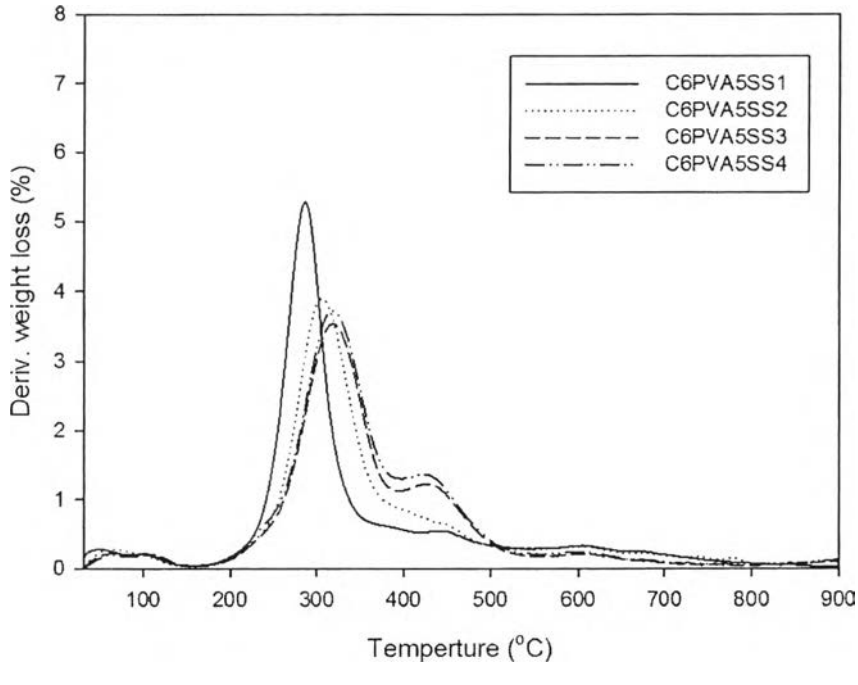

Figure 5.11 DTG thermograms of silk sericin/PVA/clay aerogels with various silk sericin contents.

Table 5.2 Effect of clay contents on thermal stability of silk sericin/PVA/clay aerogel

Samples	T_d onset (°C)	Peak decomposition (°C)	Char residual (%)	Water loss (%)
C2PVA5SS1	271.1	304.9	30.4	1.5
C4PVA5SS1	261.5	292.8	46.7	1.5
C6PVA5SS1	255.9	285.7	52.6	1.9
C8PVA5SS1	257.5	286.7	63.0	1.7

Table 5.3 Effect of silk sericin contents on thermal stability of silk sericin/PVA/clay aerogel

Samples	T_d onset (°C)	Peak decomposition (°C)	Char residual (%)	Water loss (%)
C6PVA5SS1	255.9	285.7	52.6	1.9
C6PVA5SS2	266.6	305.8	52.0	1.6
C6PVA5SS3	273.1	317.6	51.3	1.7
C6PVA5SS4	275.2	319.3	50.70	1.5

5.3.4 Mechanical properties of silk sericin/PVA/clay aerogels

Neat Na-MMT aerogel exhibited fragile material with low mechanical properties. Previous studies reported that neat Na-MMT aerogel from 5 wt% of clay exhibited initial modulus only 10 kPa (Finlay *et al.*, 2008, Gawryla *et al.*, 2008, Gawryla *et al.*, 2009 and Pojanavaraphan *et al.*, 2010). The cooperation with polymeric material was required with the purpose of overcome this limitation. The compressive stress-strain curves of silk sericin/PVA/clay aerogels are shown in Figures 5.12 and 5.13. At an initial loading, the aerogels showed the linear-elastic response. While increasing the compression load, the horizontal plateau was occurred followed by the densification region where the voids were fully collapsed

(Pojanavaraphan *et al.*, 2008, Pojanavaraphan *et al.*, 2010). Table 5.4 and 5.5 summarized the mechanical properties of silk sericin/PVA/clay aerogels. When cooperate the organic compound, in this case was silk sericin and PVA, the modulus of aerogel was improved for 10-100 times from neat clay aerogel. The clay and silk sericin contents strongly affected to the mechanical properties; increasing clay contents from 2 to 6 wt%, the initial modulus dramatically increased from 238 up to 1870 kPa due to the high reinforcing efficiency of clay bentonite. In the case of 8 wt% of clay, stiffness and initial modulus were dropped from 6 %wt of clay because the clay gel dispersion was too viscous and difficult to process resulting in an inhomogeneous dispersion of the aqueous clay gel precursor and the structure defects such as air bubbles as mentioned earlier. In the same way, increasing silk sericin vastly increased the mechanical properties of the aerogels. The increasing of polymer contents like silk sericin in the aerogels enlarged the interpenetrating co-continuous networks resulting in greatly improved in mechanical properties (Alhassan *et al.*, 2010).

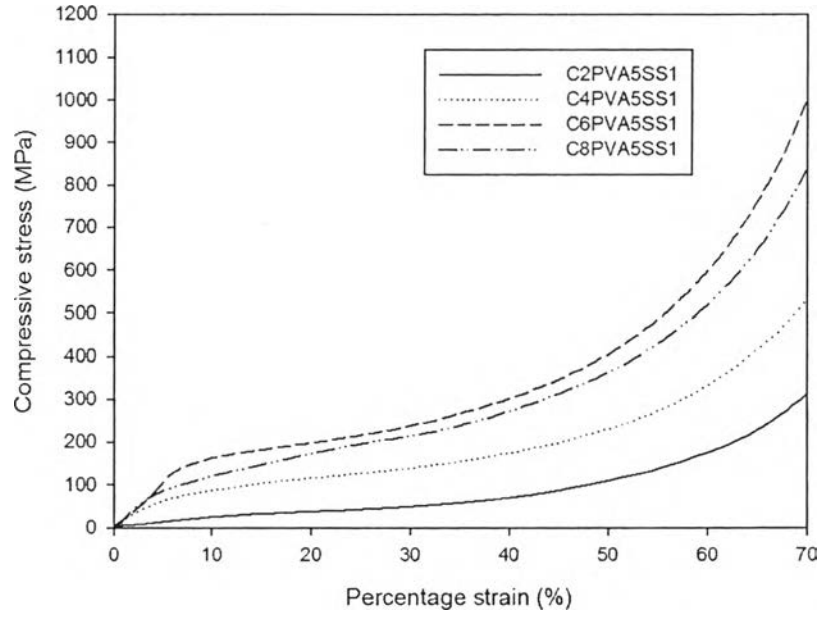

Figure 5.12 Stress-strain curves of silk sericin/PVA/clay aerogels with various clay contents.

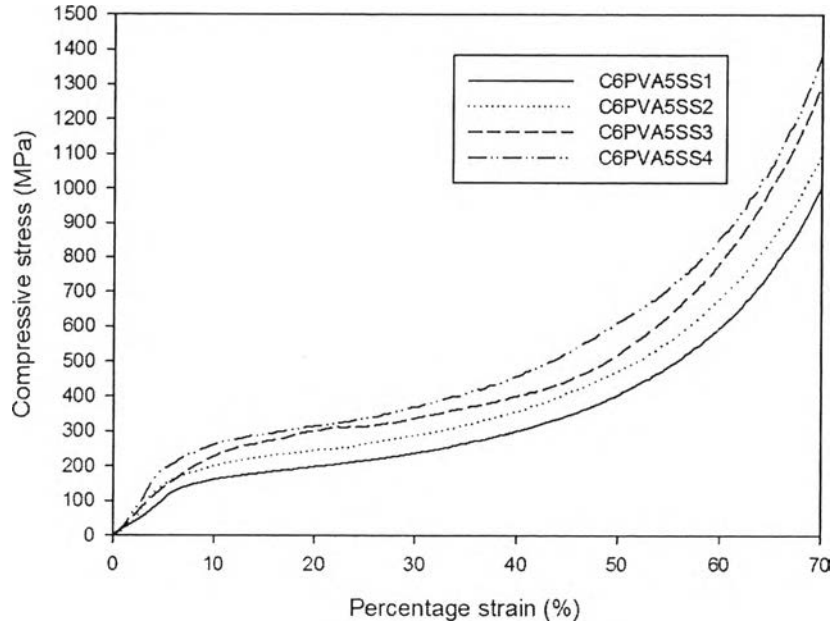

Figure 5.13 Stress-strain curves of silk sericin/PVA/clay aerogels with various silk sericin contents.

Table 5.4 Effect of clay content on mechanical properties of silk sericin/PVA/clay aerogels

Samples	Initial modulus (kPa)	Young's modulus (kPa)	Stiffness (kN/m^2)
C2PVA5SS1	238±20	2643±806	21±2.9
C4PVA5SS1	1094±232	3638±390	37±2.9
C6PVA5SS1	1870±320	5965±674	65±6.4
C8PVA5SS1	1493±130	6949±747	78±7.7

Table 5.5 Effect of silk sericin content on mechanical properties of silk sericin/PVA/clay aerogels

Samples	Initial modulus (kPa)	Young's modulus (kPa)	Stiffness (kN/m^2)
C6PVA5SS1	1870±320	5966±674	65±6.4
C6PVA5SS2	2021±203	6110±140	67±2.6
C6PVA5SS3	2753±74	7237±625	80±8.5
C6PVA5SS4	4276±473	8563±230	87±5.5

5.3.5 Dispersion of clay in silk sericin/clay/aerogels

The XRD patterns of Na-bentonite, silk sericin, PVA and silk sericin/PVA/clay aerogels are shown in Figure 5.14. The pristine Na-bentonite showed the diffraction peak at 2θ around 7.3° corresponding to a d_{001} spacing of 1.21 nm. Moreover, PVA and silk sericin showed the diffraction peaks at 2θ around 19.7° and 20.6°, respectively. The silk sericin/PVA/clay aerogels showed the reducing of the intensity of the characteristic peaks of Na-bentonite both in 001 and 100 planes due to the dilution effect by solvent, in this system was water. According to Bandi *et al.*, 2006 and Polanavaraphan *et al.*, 2010, the shifting of diffraction peaks to lower angle of bentonite aerogel composite resulting in the change in d_{001} spacing was observed. The silk sericin/PVA/clay aerogel in the composition of C6PVA5SS1 exhibited the slight decreased in the diffraction peak to the lower angle 2θ around 4° associated with d_{001} spacing of 2.21. Therefore, the intercalation of polymer within the clay palates was occurred. When the clay was swollen in solvent (water) and mixed with polymer (silk sericin and PVA), the polymer chains would be intercalated and replaced the solvent in the clay galleries resulting in the intercalation structure by solution process. Bandi *et al.*, 2006 suggested that clay in aerogel was not separately exfoliated sheet but formed in the clay bundles with the thickness around 200 nm.

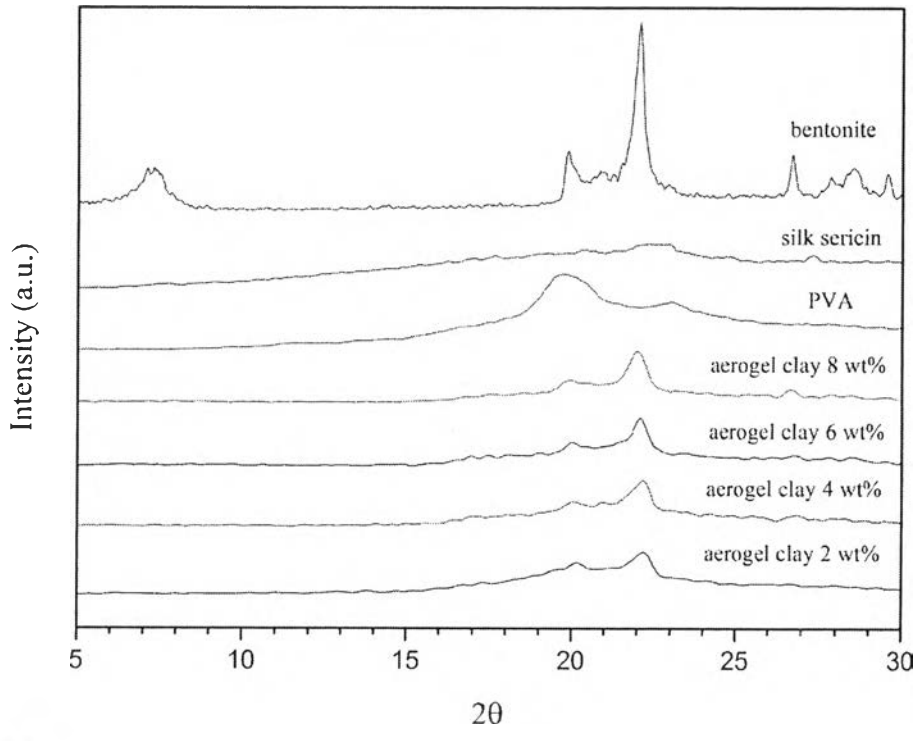

Figure 5.14 XRD patterns of Na-bentonite, silk sericin, PVA, and silk sericin/PVA/clay aerogels with various clay contents.

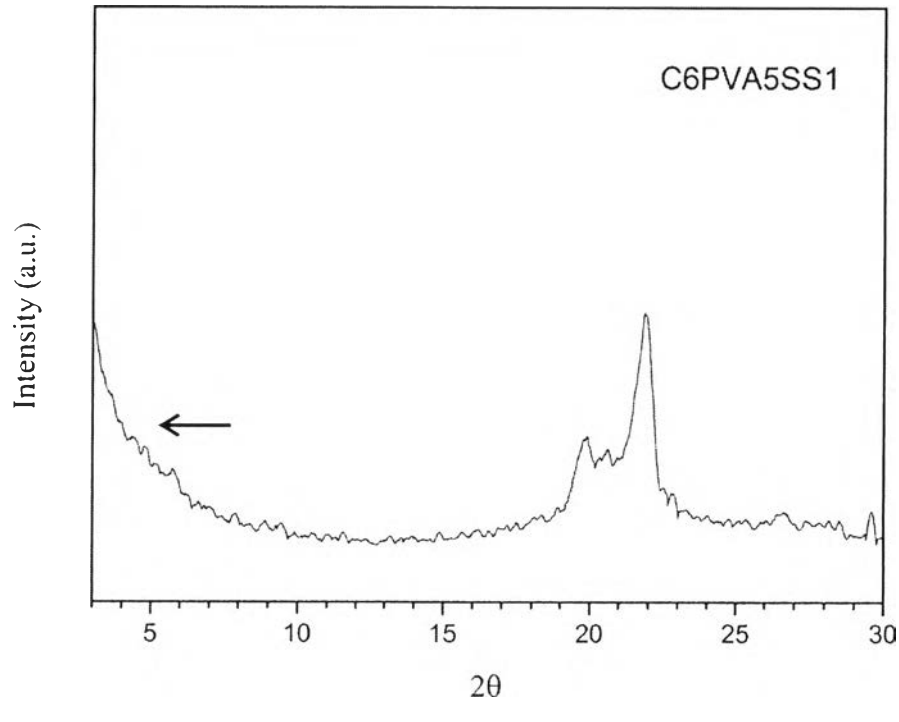

Figure 5.15 XRD pattern of silk sericin/PVA/clay aerogel with 2 theta under 5°.

5.4 CONCLUSIONS

The novel silk sericin/PVA/clay aerogel were successfully prepared by freeze-drying technique, the environmental friendly single step process. This material can be used in variety of application such as absorbent materials, insulation material, cell culture substrate, tissue engineering 3D scaffold and drug control release. The morphology and properties of the aerogels mainly depended on clay and silk sericin contents. The silk sericin/PVA/clay aerogels exhibited the highly porous and lamella morphology with interconnected pores. The mechanical properties can be improved by increasing clay and silk sericin loading. TGA studied notified that the ferric ion in clay sheet accelerated the decomposition of silk sericin/PVA resulting in the decreasing of the onset and decomposition temperature. The thermal stability can be improved by adding higher silk sericin loading. To be used as absorbent material, silk sericin/PVA/clay aerogel should be tested on the WVTR and WVP to confirm the water absorption efficiency. Additionally, biological test and swelling behavior need to be achieved in order to confirm the possibility to use for biotechnology application.

5.5 ACKNOWLEDGEMENTS

The authors would like to thank the Center of Excellence on Petrochemical and Materials Technology, Chulalongkorn University, the National Research Council of Thailand (NRCT) and the government budget 2012, for providing financial support.

5.6 REFERENCES

Alhassan, S. M., Qutubuddin, S., and Schiraldi, D. (2010) Influence of electrolyte and polymer loading on mechanical properties of clay aerogels, Langmuir, 26(14), 12198-12202.

Bandi, S. (2006) High perfomance blends and composites: part (I) clay aerogel/polymer compostes. Ph.D. Dissertation, Department of macromolecular science and engineering, Case Western Reserve University, Ohio, USA.

Haroun, A.A., Gamal-Eldeen, A., and Harding, D.R.K. (2009) Preparation, characterization and in vitro biological study of biomimetic three-dimentional gelatin-montmorillonite/cellulose scaffold for tissue engineering. Journal of Materials Science, 20, 2527-2540.

Kundu, S.C., Dash, B.C., Dash, R., and Kaplan, D. L. (2008) Natural protective glue protien, sericin bioengineered by silkworms: Potential for biomedical and biotechnological application. Progess in Polyner Science, 33, 998-1012.

Morlat, S., Mailhot, B., Gonzalez, D., and Gardette, J. L. (2004) Photo-oxidation of polypropylene/montmorillonite nanocomposites. 1. Influence of nanoclay and compatibilizing agent. Chemistry of Materials, 16, 377-383.

Pojanavaraphan, T. (2010) Layered silicate (sodium montmorillonite) based elastomer nanocomposite. Ph.D. Dissertation, The Petroleum and Petrochemical College, Chulalongkorn University, Bangkok, Thailand.

Pojanavaraphan, T. and Magaraphan, R. (2008) Prevulcanized natural rubber latex/clay aerogel nanocomposites. European Polymer Journal, 44, 1968-1977.

Pojanavaraphan, T., Schiradi, D.A., and Magaraphan, R. (2010) Mechanical, rheologinal, and swelling behavior of natural rubber/montmorillonite aerogels prepared by freeze-drying. Applied Clay Science, 50, 271-279.

Pojanavaraphan, T., Magaraphan, R., Chiou, B., and Schiradi, D.A. (2010A) Development of Biodegradable Formlike Materials Based on Casein and Sodium Montmorillonite Clay. Biomacromolecules, 11, 2640-2646.

Tassanapayak, R. (2008) Porous clay heterostructure for wastewater treatment: A development from bentonite clay in Thailand. M.S. Thesis, The Petroleum and Petrochemical College, Chulalongkorm University, Bangkok. Thailand.

Somlai, L.S., Bandi, S.A., and Schiraldi, D.A. (2006) Facile Processing of Clays into Organically-Modified Aerogels. AIChE journal, 52, 1162-1168.

Srihanam, P., Srisuwan , Y., and Simchuer ,W. (2009) Characteristic of silk fiber with and without sericin componemt: a comparison between *Bombyx mori* and *Philosamia ricini* silks. Pakistan Journal of Biological sciences, 12(11), 872-876.

Takeuchi, A., Ohtsuki, C., Kamitakahara, M., Ogata, S., Toshiki, A., Miyazaki, M., Furutani, Y., and Kinoshita, H. (2005) Biodegradation of porous alpha-tricalcium phosphate coated with silk sericin. Key Engineering Materials, 284-286, 329-332.

Teramoto, H., Kakaza, A., Yamauchi, K., and Asakura., T. (2007) Role of hydroxyl side chains in Bombyx mori silk sericin in stabilizing its solid structure. Macromolecules, 40, 1562-2569.

Zhang, Y. (2002) Applications of natural silk protien sericin in biomaterials. Biotechnology Advances, 20, 91-100.